



## Characterisation of microplastics is key for reliable data interpretation

Diana S. Moura<sup>a,\*</sup>, Carlos J. Pestana<sup>a</sup>, Colin F. Moffat<sup>a</sup>, Jianing Hui<sup>b</sup>, John T.S. Irvine<sup>b</sup>, Linda A. Lawton<sup>a</sup>

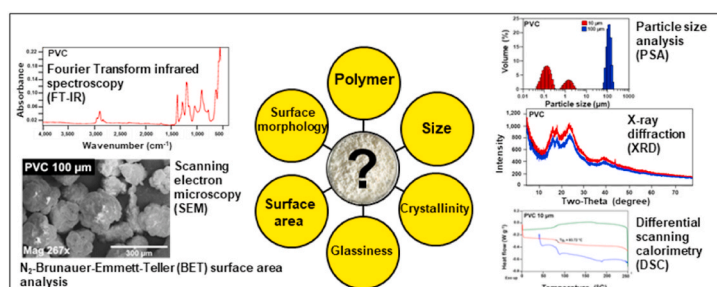
<sup>a</sup> School of Pharmacy and Life Sciences, Robert Gordon University, Aberdeen, AB10 7GJ, UK

<sup>b</sup> School of Chemistry, University of St Andrews, North Haugh, St Andrews, Scotland, KY16 9ST, UK

### HIGHLIGHTS

- Microplastics were commercially acquired as size ~20 μm (small) and ~100 μm (large).
- Information provided by the supplier was inconsistent with the analytical data produced when characterising the microplastics.
- The presence of a modifying grafting agent was detected in polypropylene (20 μm size).
- Sizes of polyamide and polyvinyl chloride were inconsistent with manufacturer's description.
- Different degrees of crystallinity were observed in 20 μm and 100 μm polyamide samples.

### GRAPHICAL ABSTRACT



### ARTICLE INFO

Handling Editor: Michael Bank

**Keywords:**  
Plastic-pollution  
Plastic characterisation  
Polymer  
Plastic particle size  
Grafting agent

### ABSTRACT

Microplastic research has gained attention due to the increased detection of microplastics (<5 mm size) in the aquatic environment. Most laboratory-based research of microplastics is performed using microparticles from specific suppliers with either superficial or no characterisation performed to confirm the physico-chemical information detailed by the supplier. The current study has selected 21 published adsorption studies to evaluate how the microplastics were characterised by the authors prior experimentation. Additionally, six microplastic types described as 'small' (10–25 μm) and 'large' (100 μm) were commercially acquired from a single supplier. A detailed characterisation was performed using Fourier transform infrared spectroscopy (FT-IR), x-ray diffraction, differential scanning calorimetry, scanning electron microscopy, particle size analysis, and N<sub>2</sub>-Brunauer, Emmett and Teller adsorption-desorption surface area analysis. The size and the polymer composition of some of the material provided by the supplier was inconsistent with the analytical data obtained. FT-IR spectra of small polypropylene particles indicated either oxidation of the particles or the presence of a grafting agent which was absent in the large particles. A wide range of sizes for the small particles was observed: polyethylene (0.2–549 μm), polyethylene terephthalate (7–91 μm) and polystyrene (1–79 μm). Small polyamide (D<sub>50</sub> 75 μm) showed a greater median particle size and similar size distribution when compared to large polyamide (D<sub>50</sub> 65 μm). Moreover, small polyamide was found to be semi-crystalline, while the large polyamide displayed an amorphous form. The type of microplastic and the size of the particles are a key factor in determining the adsorption of pollutants and subsequent ingestion by aquatic organisms. Acquiring uniform particle sizes is challenging,

\* Corresponding author.

E-mail address: [d.souza-moura1@rgu.ac.uk](mailto:d.souza-moura1@rgu.ac.uk) (D.S. Moura).

<https://doi.org/10.1016/j.chemosphere.2023.138691>

Received 17 January 2023; Received in revised form 10 March 2023; Accepted 12 April 2023

Available online 17 April 2023

0045-6535/© 2023 The Authors. Published by Elsevier Ltd. This is an open access article under the CC BY license (<http://creativecommons.org/licenses/by/4.0/>).

however based on this study, characterisation of any materials used in microplastic-related experiments is critical to ensure reliable interpretation of results, thereby providing a better understanding of the potential environmental consequences of the presence of microplastics in aquatic ecosystems.

## 1. Introduction

The increasing detection of contaminants in aquatic ecosystems is a continuing concern of many governments and inter-governmental organisations due to the consequences of the presence of contaminants on ecosystem health and thus ecosystem services. There has been a greater awareness of the issues associated with microplastics in recent years due to their increased detection in both freshwater and marine environments (Vaughan et al., 2017; Wang et al., 2018b; Xiong et al., 2018) as well as the recognition that microplastics act as a vector for chemical pollutants (Joo et al., 2021; Magadini et al., 2020). Around 3700 research publications involving microplastic pollution, published between 2018 and the end of 2022, are identified in the Web of Science database. Microplastics are defined as plastic particles smaller than 5 mm (Thompson et al., 2009). Sources include pre-production pellets, manufactured microplastics such as those commonly found in personal care products (Wagner et al., 2014) and microplastics produced by physical, chemical, and/or biological degradation (Thompson et al., 2009). A number of adsorption studies have been carried out to elucidate the impact of the microplastics in the aquatic environment. For instance, researchers have investigated the adsorption of organic compounds on microplastics (Hüffer et al., 2018; Moura et al., 2022; Pestana et al., 2021; Wagstaff et al., 2022) as well as the effect of microplastics on organisms by direct external contact (Gong et al., 2022) and by ingestion (An et al., 2021). The interaction of microplastics with contaminants present in aquatic systems and/or organisms are complex (Wang et al., 2018a). Different factors affect the adsorption of contaminants onto microplastics and ingestion of microplastics by wildlife. These include the chemistry of the contaminant, the environmental conditions, and the specific physico-chemical properties of the microplastic (Lionetto and Esposito Corcione, 2021). The microplastic type, degree of crystallinity, glassiness, polarity, and particle size can influence the adsorption behaviour of pollutants onto microplastics (Atugoda et al., 2021). Particle size, in particular, has been shown to be a key factor for adsorption of compounds by microplastics (Ma et al., 2019; Pestana et al., 2021) and directly influence ingestion of microplastics by aquatic organisms such as *Daphnia magna* (An et al., 2021).

Researchers obtain microplastics from a range of sources and in some cases prepare their own by mechanical blending (Elizalde-velázquez et al., 2020; Pestana et al., 2021; Wu et al., 2016) or grinding (Guo et al., 2018; Wu et al., 2020a) plastic pellets, and grating large pieces of plastic (Xu et al., 2018a) to obtain the microplastic particles. Typically, the particles are then sieved to obtain a specific size range that is relevant for a particular investigation. However, preparing microplastics in the laboratory is very time-consuming, presents difficulties in obtaining particles small enough and poses the risks of exposure by those undertaking the research to fine particle dust. Microplastics can be acquired commercially and are frequently used as received. This can lead to erroneous interpretation of results if the researcher assumes that the microplastics received are as described by the manufacturer with no characterisation being done prior to the experiment. The current study selected 21 published adsorption studies to evaluate how the microplastics were characterised prior to experimentation by the authors. For instance, a study aiming to evaluate the exposure of commercially acquired polystyrene (PS) beads, described as 0.1 µm and 1 µm in size, on *Microcystis aeruginosa* growth and microcystin production (Wu et al., 2021). An SEM image was used to demonstrate the effect of 1 µm PS on *Microcystis aeruginosa* cells. However, the particles highlighted by the authors as 1 µm PS beads aggregated on *M. aeruginosa* cells were in fact sized at  $0.36 \pm 0.1$  µm ( $n = 3$ , measured by the current study using

ImageJ). The number of companies that commercially supply micro-particles has increased. Due to the wide range of products available, characterisation of the microplastics used in any experiment should be an essential component of the experimental process.

This study has performed a detailed characterisation of six microplastic polymers described as 'small' (10–25 µm, according to manufacturer) and 'large' (100 µm, according to manufacturer). Experiments to confirm the polymer composition, the crystallinity pattern, the degree of crystallinity, the glassiness, the size of the particles, the surface morphology, and the surface area of polypropylene (PP), polyethylene (PE), polyethylene terephthalate (PET), polyamide (PA), polystyrene (PS), and polyvinyl chloride (PVC) were carried out and compared against the manufacturer's description of the supplied microplastics. Implications of the findings are considered of extreme value to the microplastic research field, highlighting the importance of a detailed characterisation of commercial microplastics used in microplastics-related experiments, including adsorption experiments.

## 2. Materials and methods

### 2.1. Literature overview

How microplastics are treated before being used in adsorption experiments varies widely. A number of adsorption studies ( $n = 21$ ) were selected to evaluate how the authors treated, identified and/or confirmed the physical characteristics of the microplastics as received from the supplier. The aim was to investigate whether the microplastic information provided in the selected studies aligned with the characterisation data presented. To ensure a comprehensive analysis, the current study applied the following selection criteria to identify relevant studies: (1) publication in the last five years (i.e., 2018–2022), with an exception made for highly cited studies; (2) inclusion of diverse microplastic properties data, such as polymer composition, weathering, and size. The compounds investigated, the polymer composition of the microplastics, the size of the particles as stated by the authors, the microplastic supplier, the particle size analysis performed, the scanning electron microscopy (SEM) images (if present), and the (pre-)treatment of the material received before use in adsorption experiments were assessed (Table 2, Table S1).

### 2.2. Virgin microplastic acquired commercially

Six microplastics types were commercially acquired from a single supplier. Virgin microparticles of polypropylene (PP), polyethylene (PE), polyethylene terephthalate (PET), polyamide (PA), polystyrene (PS) and polyvinyl chloride (PVC) were purchased from Shanghai Guanbu Electromechanical Technology Co. Ltd., China. The microplastic particles were acquired in two different sizes, described as small particles (10–25 µm) and large particles (100 µm). In the current study, the microplastics were labelled according to the average particle size as detailed by the supplier (Table 1).

### 2.3. Characterisation of the commercially acquired microplastic particles

The microplastic particles were characterised to confirm the specifications provided by the manufacturer. A Nicolet iS10 Fourier transform infrared (FT-IR) spectrometer (Thermo Fisher Scientific, UK) was used to confirm the chemical composition of each polymer. The FT-IR scanning wavenumber was set from 400 to 4000  $\text{cm}^{-1}$ . Attenuated total reflectance (ATR) was used to obtain the infrared spectra. Thirty-

two scans at a resolution of  $8\text{ cm}^{-1}$  were used to produce the spectra with no correction applied. FT-IR spectroscopy is a rapid, qualitative analysis capable of providing chemical structural information on a wide range of amorphous, semicrystalline and crystalline materials (Müller et al., 2014). The various spectra from the range of microplastics investigated were compared to the library on the analytical instrument (Hummel polymer sample library) and spectra presented in the literature (Geil, 2017).

The  $\text{N}_2$ -Brunauer, Emmett and Teller (BET) adsorption-desorption surface area ( $S_{BET}$ ) was determined using a Tristar II surface area and porosity instrument (Micromeritics, UK). Prior to the analysis, the microplastics were maintained under vacuum at  $30\text{ }^\circ\text{C}$  for 24 h using a VacPrep degasser (Micromeritics, UK) to remove surface-adsorbed gases and moisture. Particle size analysis (PSA) was carried out using a Mastersizer 2000 particle size analyzer (Malvern Panalytical, UK). Simulated surface area ( $S_{PSA}$ ) was calculated by the instrument modelling the particles as perfect spheres and not accounting for the porosity and roughness of the material. Scanning electron microscopy (SEM, Scios DualBeam, Thermo Fisher Scientific, UK) was used to investigate the morphologies and to confirm the particle size of the microplastics. The software ImageJ (National Institutes of Health, US) was used to measure the particle size from the SEM images in the selected studies. Snapshots of the SEM micrographs in the published studies were captured using a snip & sketch tool (Microsoft) to allow evaluation of the particle size using ImageJ. To measure the particle size, the scale bar shown in each captured image was set as the size reference. Measurements of the microplastic particles depicted in the SEM micrographs were then carried out against the scale bar reference data.

For crystallinity pattern evaluation, powder x-ray diffraction

analysis (XRD) was carried out using an Empyrean diffractometer (Malvern Panalytical, UK) in reflection mode with a primary beam monochromator (reflection mode  $\text{Cu K}\alpha 1$ ). The diffraction patterns of polymers are like fingerprints that can be compared against data in the literature for identification. The XRD pattern is a plot of the intensity of X-rays scattered at different angles by a sample (Speakman, 2021).

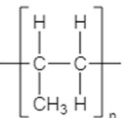
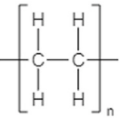
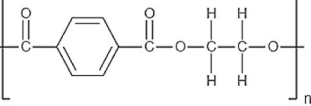
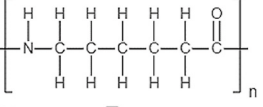
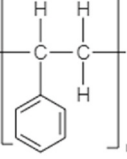
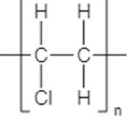
The calorimetry characteristic of the microplastics was measured by differential scanning calorimetry (DSC) using a DSC250 (TA, USA) with  $\text{N}_2$  as the purge gas. Microplastics (6.0 mg) were placed into an aluminium pan (TA, USA) and sealed with an aluminium lid using a Tzero Press (both TA, USA). The pan, lid, and samples were handled using metal forceps to avoid external interference on the samples' weight. A sample without microplastic was prepared as a reference. To erase any thermal history effects, a heating-cooling-heating method was applied. The degree of crystallinity ( $X_C$ ) was calculated using equation (1):

$$X_C = \frac{\Delta H_m - \Delta H_c}{\Delta H_{m100\%}} \times 100 \quad (1)$$

where,  $\Delta H_m$  is the enthalpy change associated to the melting endotherm temperature ( $T_m$ ) from the second heating run.  $\Delta H_c$  is the enthalpy change associated to the cold crystallisation exotherm temperature ( $T_c$ ).  $\Delta H_{m100\%}$  is the reference value considering 100% crystalline polymer. DSC analysis can identify various physical properties and thermal transitions of polymeric materials (Singh and Singh, 2022) such as the glass transitional temperature ( $T_g$ ), the melting temperature ( $T_m$ ) and the enthalpy change associated to  $T_m$  ( $\Delta H_m$ ). The melting point is the temperature at which the crystalline order is completely destroyed on heating (Chawla, 2012), whereas the  $T_g$  is the temperature at which the

**Table 1**

Average particle sizes detailed by the supplier, chemical structure (repeat unit), and polarity of polypropylene (PP), polyethylene (PE), polyethylene terephthalate (PET), polyamide (PA), polystyrene (PS), and polyvinyl chloride (PVC).

Polymer	Chemical structure (repeat unit)	Small particles - average size ( $\mu\text{m}$ )	Large particles - average size ( $\mu\text{m}$ )	Polarity
PP		25	100	Non-polar <sup>a</sup>
PE		15	100	Non-polar <sup>a</sup>
PET		15	100	Polar <sup>b</sup>
PA <sup>c</sup>		18	100	Polar <sup>a</sup>
PS		13	100	Non-polar <sup>a</sup>
PVC		10	100	Polar <sup>a</sup>

<sup>a</sup> Li et al. (2018) and.

<sup>b</sup> Seki et al. (2014).

<sup>c</sup> Polyamide 6 (nylon 6).

material becomes rubbery (soft) due to changes in chain mobility. Polymers with a  $T_g$  below ambient temperature ( $T_{amb}$ , 25 °C) are considered rubbery, while when  $T_g$  is above  $T_{amb}$ , the polymer is considered a glassy polymer. Rubbery polymers are considered to have greater adsorption potential when compared to glassy polymers (Alimi et al., 2018). Likewise, amorphous polymers are expected to show greater adsorption of organic compounds than semi-crystalline polymers (Guo and Wang, 2019). Semi-crystalline polymers can be identified by the presence of a  $T_m$  peak in DSC analysis, as well as the presence of sharp peaks in their XRD pattern.

### 3. Results and discussions

#### 3.1. Characterisation of microplastic particles in previously published research

Over 1000 publications related to the adsorption of a wide range of compounds to microplastics have been published in the past 5 years according to the Web of Science database, (2022). The adsorption of compounds such as cyanotoxins (Moura et al., 2022; Pestana et al., 2021), pharmaceuticals (Puckowski et al., 2021; Wagstaff et al., 2022; Wagstaff and Petrie, 2022), and trace metals (Turner and Holmes, 2015) onto different types of microplastics of various sizes under distinct environmental conditions has been evaluated. In a review, Alimi et al. (2018) ranked nine microplastic types according to their sorption capacity. According to the review, the microparticles of PE and PS showed the greatest adsorption of compounds compared to PP, PVC, PA, PET

**Table 2**

Summary of the selected adsorption studies ( $n = 21$ ) according to microplastic type investigated, size of the particles stated by the authors, particle size analysis (PSA), scanning electron microscopy (SEM), microplastic treatment (size-wise) prior to the experiment and weathering of the microplastics. Polypropylene (PP), polyethylene (PE), low density PE (LDPE), high density PE (UHMWPE), average density PE (AMWPE), polyethylene terephthalate (PET), polyamide (PA), polystyrene (PS), polyvinyl chloride (PVC). The particle size in the SEM images was measured using the ImageJ software. For more details see Table S1.

Microplastics type	Size ( $\mu\text{m}$ )	FT-IR	PSA	SEM	Microplastic treatment	Weathering	Reference
UHMWPE PS AMWPE PP	PP ~1000 PS 600–800 AMWPE 300–400 UHMWPE 2–10	No, but DSC and XRD	Optical microscope image	Zoom makes impossible to check the size	Blended and sieved	Virgin	Elizalde-velázquez et al. (2020)
PE PS PP PA PVC	$D_{90}$ 75-180	No, but XRD	PSA performed - no method described	Zoom makes impossible to check the size	Used as received	Virgin	Li et al. (2018)
PA PE PET PS PVC PP	100–150	None	Sieve	None	Sieved	Virgin	Guo et al. (2019)
PE	250–280	None	Sieve	None	Blended and sieved	Virgin	Wu et al. (2016)
UHMW-PE	45–48	None	SEM	SEM images show particles from 10 to 67 $\mu\text{m}$	Used as received	Virgin	Mamitiana et al. (2018)
LDPE PVC PP HDPE PE	63–125 mean size 150	None	Sieve None	None SEM images show particles from 13 to 167 $\mu\text{m}$	Sieved beads Used as received	Virgin	Puckowski et al. (2021) Xu et al., 2018b
PS Beach PS	450-1000	Yes	Sieve	Zoom makes impossible to check the size	Sieved	Aged	Zhang et al., 2018
PS PVC	mean size 75	Yes	None	Zoom makes impossible to check the size	Used as received	Aged	Liu et al., (2019)
PE	mean size 100	Yes	None	SEM images show particles from 18 to 191 $\mu\text{m}$	Used as received	Virgin	Atugoda et al. (2020)
PE PS PP	<280	None	Sieve	SEM images show: for PE from 13 to 66 $\mu\text{m}$ for PP from 19 to 236 $\mu\text{m}$ for PS from 13 to 171 $\mu\text{m}$	Grated and sieved	Virgin	Xu et al., 2018a
PE PP PS PVC	<74	Yes	Sieve	One particle	Grinded and sieved	Virgin	Guo et al. (2018)
PLA PVC	PLA 250–550 PVC 75–150	Yes	None	SEM images show: for PLA 250 $\mu\text{m}$ for PVC 76 $\mu\text{m}$	Used as received	Aged	Fan et al. (2021)
PVC PP PE	4000–5000	None	Stereomicroscopic image	None	Used as received	Virgin	Lu et al. (2020)
PS	mean sizes 75.4106.9150.5214.6	Yes	Laser particle size analyser	Zoom makes impossible to check the size	Sieved	Virgin	Li et al. (2019)
PVC	Small <1 Large ~100	Yes	SEM	SEM images show: For small from 0.19 to 1.00 $\mu\text{m}$ For large from 64 to 244 $\mu\text{m}$	Used as received	Virgin	Ma et al. (2019)
PE PS soil	PE 225 $\pm$ 41 PS 313 $\pm$ 48 Soil <74	Yes	SEM	One particle	Used as received	Virgin	Chen et al. (2021)
PP	<180	Yes	Laser particle analyser - no particle distribution shown	One particle	Grinded and sieved	Aged	Wu et al. (2020)
PS	50.4 $\pm$ 11.9	Yes	SEM	One particle	Used as received	Aged	Liu et al. (2020)
PE PS PP PA PVC	<250	None	Laser light shading and simultaneous microscopy	None	Sieved	Virgin	Hüffer and Hofmann (2016)
PS	4000	Yes	None	Zoom makes impossible to check the size	Used as received	Aged	Wu et al. (2020a)



and polyoxymethylene. PE (including low, average, high density, and non-specified PE) and PS were the microplastic types most studied across the reviewed literature ( $n = 21$ , Table 2, Fig. 1).

In contrast, PET and polylactic acid (PLA) were the type of microplastic least studied. Throughout the studies analysed, 38% of authors evaluated a single type of microplastic in contact with organic compounds. Just over one half (52%) of the adsorption studies included in this review used the particles as received from the supplier of which one checked the size of the particles (Table 2). Throughout the studies that used the particles as received (11), Li et al. (2018) was the only one to use a particle size analyser to verify the size of the microplastics, however, neither the instrument nor the method used were described by the authors.

The remaining studies analysed the particles using images from a scanning electron microscope (SEM) to confirm the size of the acquired particles. However, visual analysis of the particle size using SEM images has limitations. For instance, nine studies show the SEM images either of one single particle or zoomed in on a single particle making it impossible to assess the size-distribution of particles in a given sample (Chen et al., 2021; Elizalde-velázquez et al., 2020; Fan et al., 2021; Guo et al., 2018; Li et al., 2018; Liu et al., 2019; 2020; Wu et al., 2020b; Zhang et al., 2018). Although SEM images taken at high magnification are important to elucidate the surface morphology of the microplastics, it makes it impossible to assess the particle size distribution. When the microplastics were sieved, the studies tend to rely on the pore size of the sieves used to describe the particle size range (Guo et al., 2019, 2018; Pestana et al., 2021; Puckowski et al., 2021; Wu et al., 2016; Zhang et al., 2018). Sieving the microplastics received was used as the only particle size control by 29% of the studies (Guo et al., 2019, 2018; Puckowski et al., 2021; Wu et al., 2016; Xu et al., 2018a; Zhang et al., 2018). Studies presented a mean particle size to identify a range of sizes while small plastics debris was ignored. For instance, in a study investigating the adsorption behaviour of the antibiotic sulfamethoxazole onto PE, a median size of 150  $\mu\text{m}$  was quoted. However, when analysing the SEM image of the PE particles present in the study (measured by the current study using ImageJ), the particle size varied between 13 and 167  $\mu\text{m}$  (Xu et al., 2018a). Likewise, in a study which evaluated the adsorption of the antibiotic Ciprofloxacin onto PE at a median size of 100  $\mu\text{m}$ , the SEM image showed particles ranging in size from 18 to 191  $\mu\text{m}$  (measured by

the current study using ImageJ, Atugoda et al., 2020). Similarly, in a study that investigated the adsorption of the pharmaceuticals sulfamethoxazole, propranolol, and sertraline onto PE, the authors reported a size range from 45 to 48  $\mu\text{m}$ . However, the published SEM image showed the size of the particles to range from 10 to 67  $\mu\text{m}$  (measured by the current study using ImageJ, Mamiñana et al., 2018).

Acquiring a uniform particle size is a challenge, however the size distribution of the particles is critical because the size of the microplastics has been shown to be a key factor in respect of the adsorption of compounds on microplastics (Li et al., 2019; Moura et al., 2022; Pestana et al., 2021). Among the studies investigated ( $n = 21$ ), 38% (8) did not check in any way the polymer composition of the plastic received from the supplier. In two studies some analyses, including DSC or XRD, were used to characterise the particles prior to experimentation (Elizalde-velázquez et al., 2020; Li et al., 2018). Most of the studies that performed FT-IR analysis focused on evaluating the aging of the polymer rather than confirming the polymer composition and purity of the microplastics.

### 3.2. Thorough characterisation of commercially acquired microplastics

#### 3.2.1. Identification of polymers

In the current study, microparticles of six different polymer materials were acquired commercially in two sizes to evaluate whether the information provided by the supplier matched with the analytical data produced. The polymer composition of the microplastics is an important factor in determining the adsorption of organic compounds (Guo et al., 2019; Hüffer and Hofmann, 2016). Depending on the microplastic type (polymer-based) different adsorption mechanisms are involved in the adsorption of organic compounds (Atugoda et al., 2021). These can affect the amount adsorbed and the desorption potential of microplastics. FT-IR spectroscopy was performed to confirm the chemical nature of the constituent polymers of the commercially acquired microplastics that were to be used by the authors to investigate adsorption of a range of chemicals. The FT-IR spectra provides a fingerprint for each of the polymers. The FT-IR spectra can be compared with those in a library to either identify or confirm the polymeric material. The polymer composition of the 6 microplastics matched with the description supplied by the manufacturer. The various spectra from the

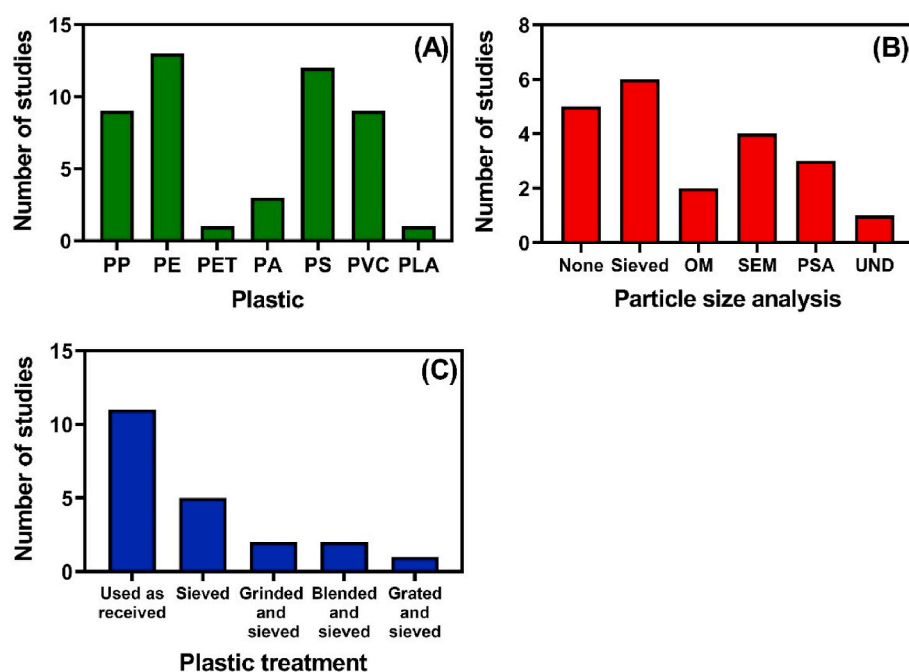


Fig. 1. Number of adsorption studies grouped by (A) plastic, (B) particle size analysis, and (C) treatment of the microplastics (regarding size) before experiment ( $n = 21$ ). Polypropylene (PP), polyethylene (PE), polyethylene terephthalate (PET), polyamide (PA), polystyrene (PS), polyvinyl chloride (PVC), and polylactic acid (PLA). Optical microscope (OM), scanning electron microscope (SEM) images, particle size analyser (PSA). Undefined (UND) means that particle size analysis was performed, but the method was not mentioned by the authors. Supplier origin was considered *not informed* (NI) when either the authors did not mention the company name or did not specify the country of origin for the company (for more details see Supplementary Information Table S1).

range of microplastics being investigated matched the library on the analytical instrument (Hummel polymer sample library) and spectra presented in the literature (Geil, 2017). Further evaluation of the FT-IR spectra of the microplastics can include the identification of functional groups based on the spectral position of the peaks (wavenumbers). PP and PE consist of the alkane (C–C and C–H) functional groups (Table 1).

These result in a strong absorption band between 3000 and 2840  $\text{cm}^{-1}$ . Corresponding peaks were present in the spectra of the polymers described at purchase as PP and PE (Fig. 2). No differences were apparent for the spectra of the two sizes of PE (described by the supplier as being of sizes 15  $\mu\text{m}$  and 100  $\mu\text{m}$ ). However, a peak corresponding to the carbonyl functional group (C=O) was present in the spectrum of the

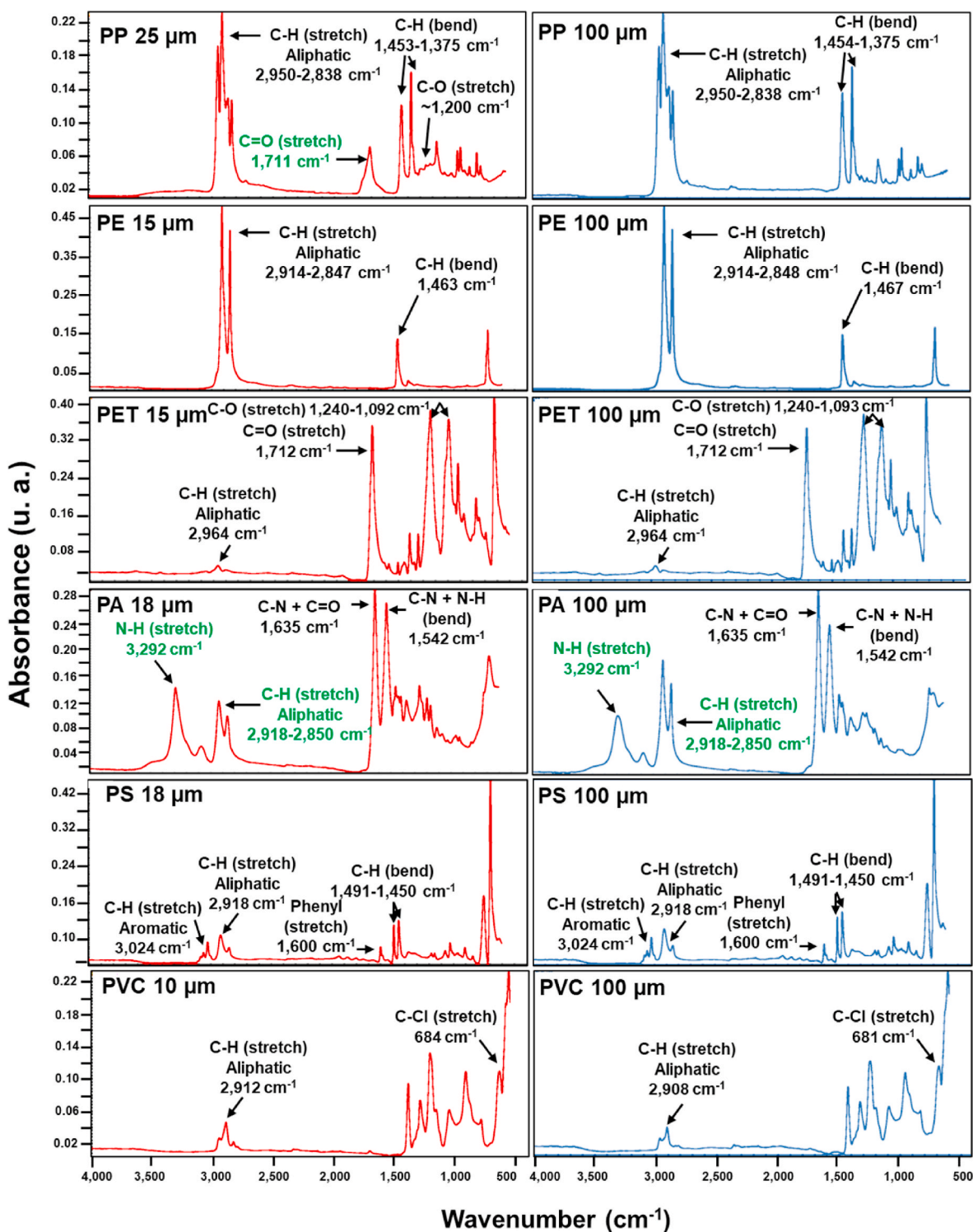


Fig. 2. Attenuated total reflectance Fourier transform infrared (ATR FT-IR) spectra of polypropylene (PP), polyethylene (PE), polyethylene terephthalate (PET), polyamide (PA), polystyrene (PS), and polyvinyl chloride (PVC) described at time of purchase as small (10–25  $\mu\text{m}$ , red) and large (100  $\mu\text{m}$ , blue). PP, PE, PET, PA, PS, and PVC main functional groups and their FT-IR absorption peaks are presented. Chemical structures of the plastics are presented in Table 1. The sizes are as supplied by the manufacturer. Highlighted in green are the FT-IR peaks that showed difference between the small and large size.

small PP. No such peak was observed in the large PP spectra (Fig. 2). The presence of a carbonyl peak in the spectrum of small PP can be associated with either oxidised particles of PP or the presence of a grafting agent. Grafting polymerisation is a popular method for the modification of shape, size, and structure of polymeric materials (Mandal et al., 2017). Grafting agents such as acrylic acid and maleic anhydride are organic compounds containing carbonyl groups. Acrylic acid is used mainly in the composition of polymers, including plastics (Brown, 2014) such as polyacrylic acid. The strong, sharp peak in the small PP FT-IR spectrum at  $1711\text{ cm}^{-1}$  and the weak peak at  $1200\text{ cm}^{-1}$  correspond to the carboxylic acid (RCOOH) and C–O (stretch) peak, respectively (Fig. 2). The presence of these FT-IR peaks might indicate a grafting reaction of acrylic acid (AA) on PP forming the copolymer known as PP-g-AA (Cai et al., 2008; Mandal et al., 2017; Xu et al., 2014). Acrylic acid is an unsaturated carboxylic acid that has a characteristic acidic and tart aroma at room temperature. A strong acidic and tart smell was also observed by the authors of this study when handling the small PP samples. These characteristics are indicative of the presence of grafting agents, but it was not possible to make a definitive identification. Nevertheless, the different chemical structure of small PP will impact the adsorption behaviour of organic compounds on this PP as demonstrated by Moura et al. (2022). The authors observed significant adsorption of a cyanotoxin and its variants (microcystins) on small particles of this PP which was characterised by the presence of the carbonyl functional group in the FT-IR spectrum.

A strong peak at  $1712\text{ cm}^{-1}$  was observed in both the small and large PET FT-IR spectra. In this case, the peak is consistent with the ester functional group (RCOOR) which is present in PET (Table 1). Furthermore, both small and large particles of the polyester, PET, showed matching spectra. The FT-IR spectra of the small and large sizes of PA demonstrated distinct peaks for N–H ( $3292\text{ cm}^{-1}$ ) and C–H ( $2918\text{--}2850\text{ cm}^{-1}$ ) stretching frequencies. There were, however, differences including the higher absorbance intensity of the N–H peaks in the spectra of small PA (0.14 u.a) compared to in the large PA (0.11 u.a). Likewise, the lower absorbance intensity of C–H peaks in the small PA spectrum (0.12 u.a) in contrast to large PA spectrum (0.18 u.a). These might indicate that the material described as small and large PA are two different forms of PA. Depending on the arrangement and chemical nature of the monomers, PA can be classified into various categories, such as aromatic, cycloaliphatic, and aliphatic PA (Kausar, 2017). The FT-IR spectra cannot, on their own, be used to precisely identify the form of PA present in the sample, therefore further characterisation would be required to confirm the specific form present.

PS and PVC both showed matching spectra for the two sizes acquired. The aliphatic C–H stretching adsorption peak ( $\sim 2910\text{ cm}^{-1}$ ) is present in both the PS and PVC spectra, but the aromatic C–H stretching peak ( $3024\text{ cm}^{-1}$ ) is only observed in the PS spectra (Table 1, Fig. 2). On the other hand, PVC has chlorine related absorptions (C–Cl peak) at  $684\text{ cm}^{-1}$  (10  $\mu\text{m}$  particles) and  $681\text{ cm}^{-1}$  (100  $\mu\text{m}$  particles).

### 3.2.2. Verification of the size distribution

In addition to the polymer that makes up the particles, the size of the microplastics has been found to be a key factor for adsorption of micropollutants on plastic particles (Pestana et al., 2021). Smaller particles have a greater surface area than larger particles, therefore greater adsorption is expected (Chen et al., 2013). However, few studies verify the size of the particles as received from the supplier. Due to the importance of the microplastic size for data interpretation, particle size analysis (PSA) was performed in the commercial microplastics acquired to determine the median size ( $D_{50}$ ) and the size distribution of the material received. In the current study, the size of the particles acquired was, in general, inconsistent with the size data provided by the supplier. An extreme example was the small PA. The material was described as having an average size of 18  $\mu\text{m}$ . When analysed, the  $D_{50}$  was determined to be 75  $\mu\text{m}$  (Table 3). Small PA showed a similar size distribution to large PA ( $D_{50}$  65  $\mu\text{m}$  compared to 100  $\mu\text{m}$  as detailed by the supplier,

**Table 3**

Particle size analysis (PSA) range, PSA median of the particle size distribution ( $D_{50}$ ) of polypropylene (PP), polyethylene (PE), polyethylene terephthalate (PET), polyamide (PA), polystyrene (PS), and polyvinyl chloride (PVC) described as small (10–25  $\mu\text{m}$ ) and large (100  $\mu\text{m}$ ) by the supplier. \*Note: There are two PSA ranges for PVC due to the fact that on analysis there were found to be two distinct size distributions.

Plastic – ‘small’ particles	Average size detailed by the supplier ( $\mu\text{m}$ )	Results from this study	
		PSA range* ( $\mu\text{m}$ )	$D_{50}$ ( $\mu\text{m}$ )
PP	25	4–23	8
PE	15	0.2–549	25
PET	15	7–91	28
PS	13	1–79	21
PA	18	0.2–363	75
PVC	10	0.04–0.3	0.11
		0.5–4	1.3

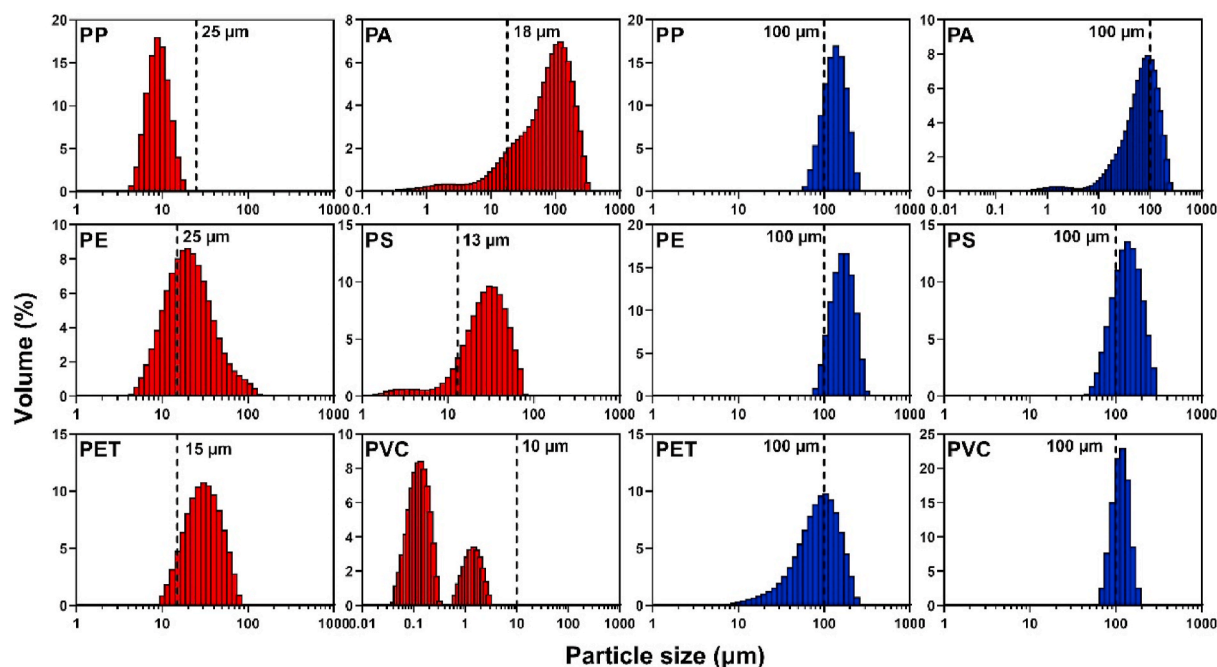
Plastic – ‘large’ particles	Average size detailed by the supplier ( $\mu\text{m}$ )	PSA range ( $\mu\text{m}$ )	
		PSA range ( $\mu\text{m}$ )	$D_{50}$ ( $\mu\text{m}$ )
PP	100	60–275	124
PE	100	69–316	153
PET	100	4–240	81
PA	100	0.3–240	65
PS	100	40–317	125
PVC	100	60–209	106

Fig. 3). In addition, the small PVC, described as having an average size of 10  $\mu\text{m}$ , showed two distinct size distributions containing particles between 0.04–0.3 and 0.5–4  $\mu\text{m}$  (Table 3, Fig. 3). Considering the results of the current investigation, combined with the fact that just over half (52%) of the adsorption studies reviewed used particles as received from the supplier with only one study performing particle size analysis, there must be significant concern regarding interpretation of adsorption data for microplastics (Fig. 1).

The extremely small size of the PVC particles (contrary to the information provided by the supplier) is of concern (Table 3). In adsorption experiments, the liquid phase is filtered to remove the microplastics before analysis of compound concentration by either injecting it into the HPLC injection port (Li et al., 2018; Puckowski et al., 2021) or photo spectrophotometer (Atugoda et al., 2020; Liu et al., 2019; Ma et al., 2019). Frequently, membranes with a pore size of 0.22  $\mu\text{m}$  or greater are used (Wu et al., 2016; Yu et al., 2020), which may be unsuccessful in removing particles smaller than 0.22  $\mu\text{m}$ . For liquid chromatographic analysis, this can result in damage to the analytical equipment. While, for photo spectrophotometer analysis, the remaining very small particles might affect absorption of the light and impact on the results. It was also observed that the small particles of PE (0.2–549  $\mu\text{m}$ ), PET (7–91  $\mu\text{m}$ ), and PS (1–79  $\mu\text{m}$ ) showed a wide size distribution that overlapped with the size distribution of the large particles (Fig. 3). The broad distribution of particle sizes would make meaningful evaluation of the impact of particle size on adsorption difficult.

Scanning electron microscope (SEM) imaging showed that the commercially acquired microplastics have mostly irregular surface morphologies (Fig. 4). The more irregular the surface of the microplastics, the greater the expected adsorption (Razanajatovo et al., 2018). Furthermore, irregular shaped particles have shown greater ecotoxicological effects on aquatic organisms (Schwarzer et al., 2022). By visually analysing the SEM images it is possible to confirm the size of the particles determined through PSA (Fig. 3). SEM images demonstrated a wide range of sizes in the samples of large PET and small PA (Fig. 4). Further, SEM images confirmed the wide range of sizes of the small PVC sample, described by the supplier as 10  $\mu\text{m}$ . Additionally, SEM images also confirmed the large actual size of small PA observed in the PSA (Fig. 3). In regard to surface morphology, a rough surface was observed for small PP and PVC, and both sizes of PE, PET, PS and PA (both sizes), as well as large PP, were characterised by smooth surfaces (Fig. 4). The difference between the surface morphologies of small PP (rough) and





**Fig. 3.** Particle size distribution from the laser diffraction particle size analysis of polypropylene (PP), polyethylene (PE), polyethylene terephthalate (PET), polyamide (PA), polystyrene (PS) and polyvinyl chloride (PVC). red = 'small' particles; blue = 'large' particles. The vertical dashed line represents the particle size as described by the supplier.

large PP (smooth) might be associated with the presence of the carbonyl functional group in the FT-IR spectra of small particles of PP which, together with the detected aroma, was indicative of the presence of a grafting agent. Mandal et al. (2017) observed that the presence of carboxylic groups on the surface of the grafted PP (PP-g-AA) film increased the roughness on the surface of PP compared to neat PP.

Small PVC was characterised as a spherical shape with a spongy looking surface. The spongy surface morphology, combined with the small particle size of the material, suggests that this material has a good potential to adsorb organic compounds. PVC particles used in a study conducted by Ma et al. (2019) showed very similar particle size and particle morphology when compared to the PVC particles in this study. The PVC particles in the study by Ma et al. were acquired from a different supplier from the current study (Dongguan Jing Tian Raw Materials of Plastics Co. Ltd., China).

### 3.2.3. Evaluation of the surface area

The surface area of the microplastics plays an important role with respect to the interaction between organic compounds and microplastics. The greater the surface area of the material, the greater the amount of binding sites potentially available for adsorption of compounds onto microplastics, therefore greater adsorption is expected. Small PP had a very high surface area ( $S_{BET}$ )  $52.2 \text{ m}^2 \text{ g}^{-1}$  compared to the other microplastics investigated during the current study (Table 4). The simulated surface area ( $S_{PSA}$ ), as determined by PSA, of small PP ( $0.72 \text{ m}^2 \text{ g}^{-1}$ ) was much lower compared to its  $S_{BET}$  which indicates that small PP is a porous material.

The increased surface area might be attributed to the grafting process of small PP as demonstrated by Yang et al. (2013). The authors showed a positive correlation between the graft ratio and the specific surface area of PP particles (Yang et al., 2013). Moura et al. (2022) performed an experiment with a mixture of eight cyanotoxin (microcystins) variants placed in contact with the same small particles and large PP and PET particles investigated in the current study. The authors demonstrated a significant adsorption of microcystins on small PP (with a carbonyl functional group peak as determined by FT-IR) when compared to small PET. In contrast, no distinct difference was observed comparing the

adsorption of large PP (without carbonyl functional group IR peak) compared to large PET.

Except for small PVC, all simulated surface areas calculated based on the particle size analysis ( $S_{PSA}$ ) were smaller than the  $S_{BET}$ , suggesting a degree of porosity/roughness for most of the microplastic particles. The average size of the smaller PVC particles was  $0.48 \text{ }\mu\text{m}$ , its  $S_{PSA}$  was  $43.5 \text{ m}^2 \text{ g}^{-1}$  while its  $S_{BET}$  was  $4.33 \text{ m}^2 \text{ g}^{-1}$  (Table 4). The reason for this observation may be that the degassing of the  $\text{N}_2$ -BET adsorption-desorption analysis was performed at  $30 \text{ }^\circ\text{C}$ , instead of the normally employed  $130 \text{ }^\circ\text{C}$ , due to the low melting points of these plastics. Occasionally, during the  $\text{N}_2$ -BET adsorption-desorption analysis, the  $\text{N}_2$  adsorbs onto the material surface, preventing full removal of  $\text{N}_2$  during the degassing step. Moreover, the degassing process removes potential gases adsorbed on the surface of the particles prior to contact with  $\text{N}_2$ , which, if unsuccessfully removed, decreases the amount of binding sites for  $\text{N}_2$ . A higher degassing temperature could not have been applied to PVC due to its glass transition temperature ( $T_g$ ; the temperature at which the plastic becomes rubbery) of  $83 \text{ }^\circ\text{C}$  (Table 4, Fig. 6). Furthermore, the aggregation of the particles during the analysis can affect the  $S_{BET}$  measured. The particles can clump, which increases the surface area of the microplastics. The  $S_{BET}$  analysis is performed using dry samples, therefore a particle dispersant cannot be used to avoid the aggregation of the particles. As expected, the  $S_{BET}$  of PA of both sizes were similar, since small and large PA are effectively the same size.

### 3.2.4. Evaluation of the crystallinity and glassiness

Amorphous polymers, in which crystalline regions are absent, are expected to show greater adsorption when compared to more crystalline polymers (Seo et al., 2022). The crystallinity pattern of the microplastics was evaluated using an x-ray diffraction (XRD) analysis. The greater the magnitude/peak height/area under the peak of the XRD pattern, the more crystalline regions on the material (Fig. 5). The XRD patterns of PP, PE, and PET showed sharp peaks with a bumpy baseline (Fig. 5), which indicates the presence of both crystalline and amorphous regions. The presence of  $T_m$  peaks confirmed the semi-crystalline structure of PP, PE, and PET (Fig. 6). On the other hand, the amorphous structure of PS and PVC was confirmed by the absence of diffraction peaks in their

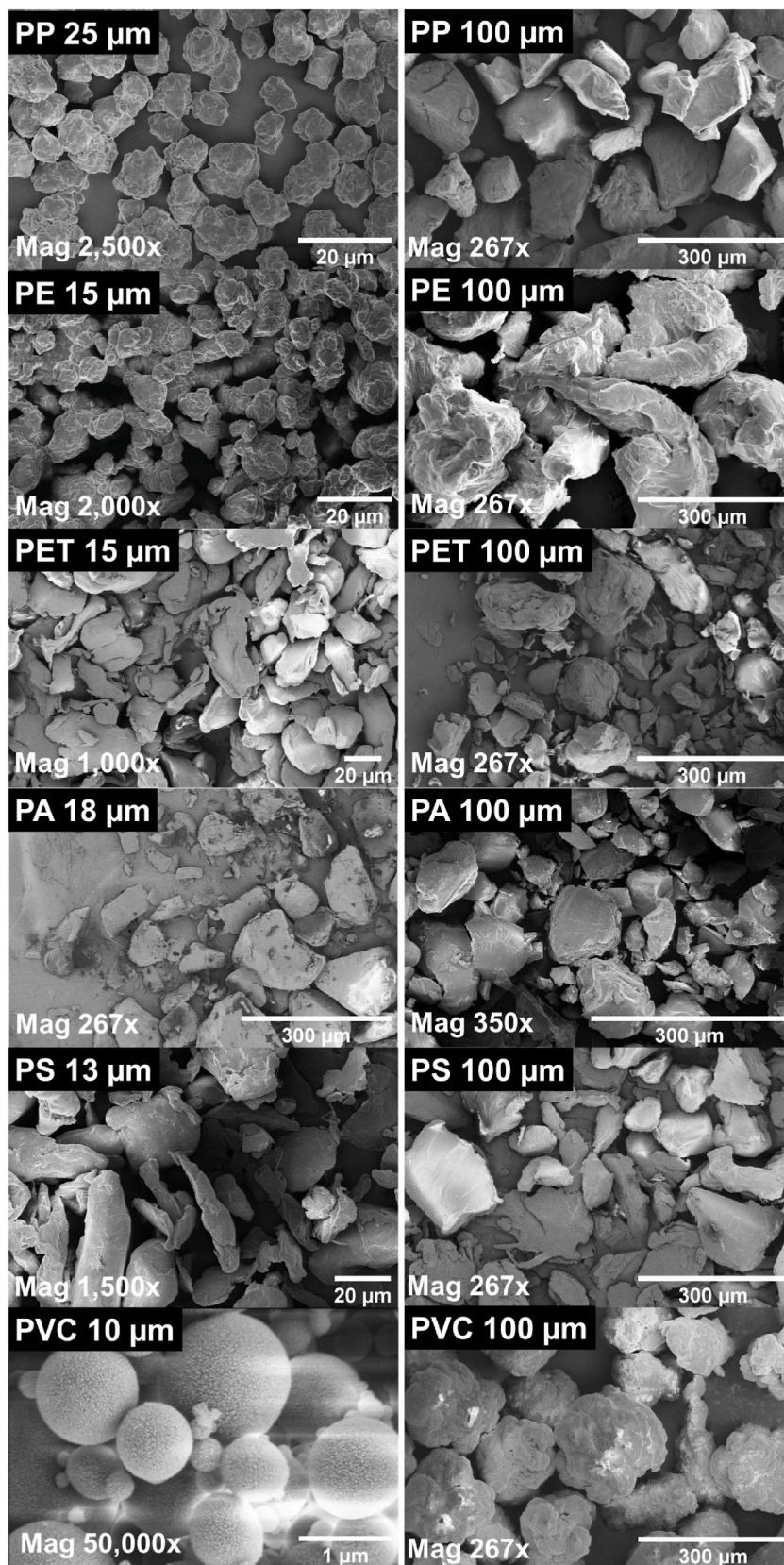


Fig. 4. Scanning electron microscope (SEM) images of polypropylene (PP), polyethylene (PE), polyethylene terephthalate (PET), polyamide (PA), polystyrene (PS), and polyvinyl chloride (PVC) with the sizes as provided by the supplier in the top left corner of each image. The magnification of the images ranged from 297x to 50,000x.



**Table 4**

Simulated surface area ( $S_{PSA}$ ), and  $N_2$ -BET adsorption-desorption surface area ( $S_{BET}$ ) of polypropylene (PP), polyethylene (PE), polyethylene terephthalate (PET), polystyrene (PS), polyamide (PA) and polyvinyl chloride (PVC) described as small (10–25  $\mu\text{m}$ ) and large (100  $\mu\text{m}$ ) by the supplier.

Plastic – ‘small’ particles	Average size detailed by the supplier $\mu\text{m}$	Results from this study	
		$S_{PSA}$	$S_{BET}$
		area $\text{m}^2$ $\text{g}^{-1}$	area $\text{m}^2$ $\text{g}^{-1}$
PP	25	0.72	52.2
PE	15	0.22	1.58
PET	15	0.31	0.82
PS	13	0.37	2.34
PA	18	0.11	0.97
PVC	10	43.5	4.33
Plastic – ‘large’ particles	Average size detailed by the supplier $\mu\text{m}$	$S_{PSA}$	$S_{BET}$
		area $\text{m}^2$ $\text{g}^{-1}$	area $\text{m}^2$ $\text{g}^{-1}$
		PP	100
PE	100	0.04	0.28
PET	100	0.10	0.46
PA	100	0.09	0.92
PS	100	0.05	0.39
PVC	100	0.06	0.59

respective XRD patterns (Fig. 5) and  $T_m$  in DSC analysis (Fig. 6). Usually, the  $T_g$  is considered the melting point of amorphous polymers. Of concern was that small PA was found to be a different form of PA when compared to large PA. The different FT-IR spectra of the two PA sizes was an indication that the small and large PA particles did not consist of the same material (Fig. 2), which was confirmed by the XRD patterns (Fig. 5) and the DSC analysis (Table 5, Fig. 6). The material described by the supplier as PA with an average size of 18  $\mu\text{m}$  (small PA), is a

semi-crystalline form of PA (Table 5). On the other hand, the absence of a  $T_m$  peak demonstrated that large PA consists of an amorphous form of PA (Table 5, Fig. 6). The  $T_m$  of small PA (221  $^\circ\text{C}$ ) matches with polyamide-6 (PA6) also known as nylon 6 (Hamid et al., 2013). Small PA was also found to be rubbery ( $T_g < 0$   $^\circ\text{C}$ ) which is consistent with PA6 (Crawford and Quinn, 2017; Guo et al., 2019). The difference in the crystallinity between the two PA sizes, and the incorrect size observed for small PA particles will lead to erroneous data interpretation in an adsorption experiment using these microparticles.

PP also demonstrated a difference between the XRD pattern of small and large particles. The higher baseline of the large particles indicates a lower degree of crystallinity compared to small PP (Fig. 5). Contrary to the observations of the XRD analysis, DSC showed that large PP has a greater degree of crystallinity (47%) compared to small PP (32%, Table 5). According to Lima et al. (2002) the discrepancy between the XRD and DSC results can be due to the thermal history of the polymer. The degree of crystallinity is calculated considering the melting enthalpy of the second heating run where the thermal history of the polymer has been erased (equation (1)). Considering the first heating run, small PP demonstrated a greater melting enthalpy peak compared to large PP (Fig. 6) which is consistent with the XRD result. Furthermore, small PP showed a lower  $T_m$  (145  $^\circ\text{C}$ ) compared to large PP (161  $^\circ\text{C}$ , Table 5, Fig. 6). The difference in both  $X_C$  and  $T_m$  for small and large PP is also an indication of the presence of acrylic acid as a grafting agent in small PP particles. Mandal et al. (2017) has demonstrated that the crystallinity of grafted PP films decreases with an increase in grafting because of the presence of acrylic acid. According to Mandal et al. (2017),  $T_m$  of the grafted PP decreased due to the grafting destroying the ordered structure of the PP crystals.

#### 4. Characterisation of microplastics recommendations prior to experimentation

The current study has clearly demonstrated that the information

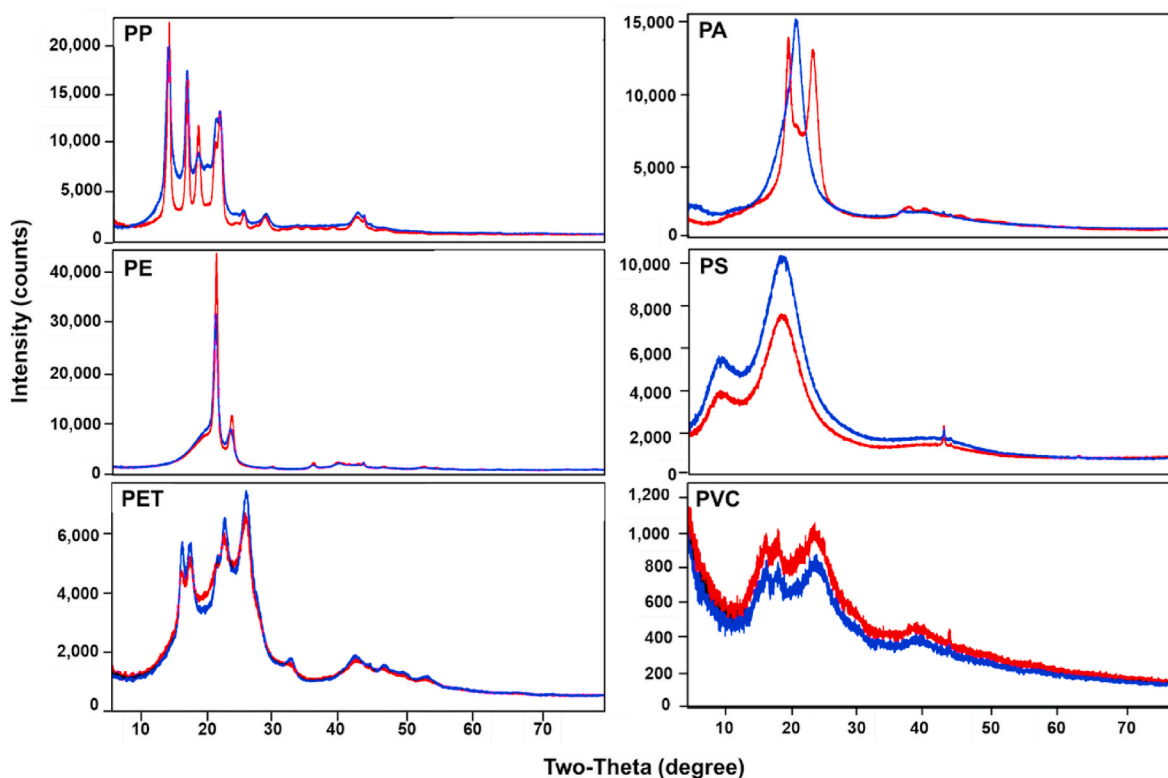


**Fig. 5.** X-Ray diffraction (XRD) pattern of polypropylene (PP), polyethylene (PE), polyethylene terephthalate (PET), polyamide (PA), polystyrene (PS), and polyvinyl chloride (PVC), red = small and blue = large. The sizes descriptions are as supplied by the manufacturer.

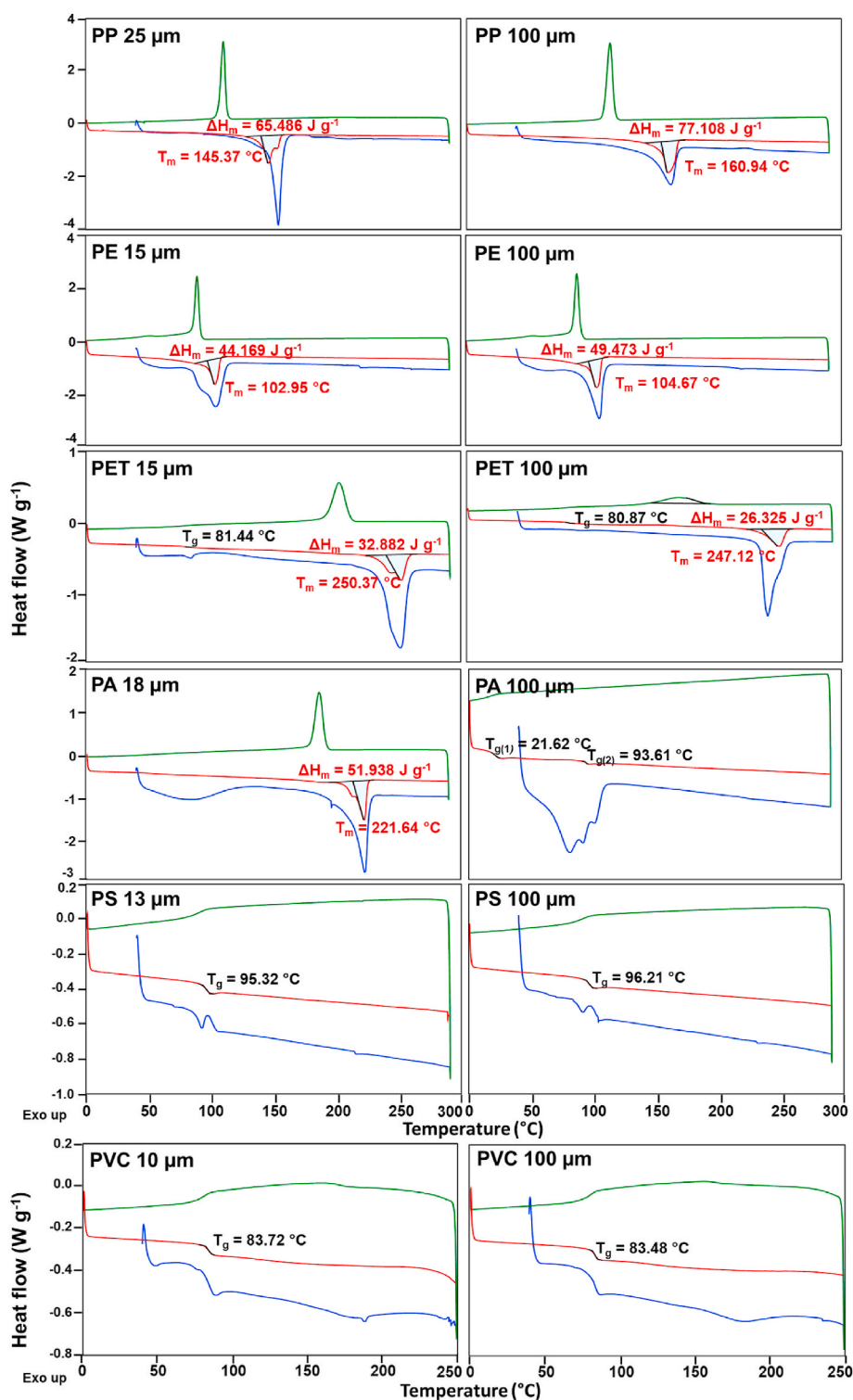


Fig. 6. Differential scanning calorimetry (DSC) of polypropylene (PP), polyethylene (PE), polyethylene terephthalate (PET), polyamide (PA), polystyrene (PS), and polyvinyl chloride (PVC). There were two primary descriptions of size made by the supplier: small (10–25  $\mu\text{m}$ ) and large (100  $\mu\text{m}$ ). For PP, PE, PET, PA, and PS, first heating run, 40–290  $^{\circ}\text{C}$  at 20  $^{\circ}\text{C min}^{-1}$  (blue), cooling run, 290–0  $^{\circ}\text{C}$  at 10  $^{\circ}\text{C min}^{-1}$  (green), and second heating run 0–290  $^{\circ}\text{C}$  at 10  $^{\circ}\text{C min}^{-1}$  (red). For PVC, first heating run, 40–250  $^{\circ}\text{C}$  at 20  $^{\circ}\text{C min}^{-1}$  (blue), cooling run, 250–0  $^{\circ}\text{C}$  at 10  $^{\circ}\text{C min}^{-1}$  (green), and second heating run 0–250  $^{\circ}\text{C}$  at 10  $^{\circ}\text{C min}^{-1}$  (red).  $\text{N}_2$  was used as the purge gas.  $T_g$  represents the glass transition temperature ( $^{\circ}\text{C}$ ), and  $\Delta H_m$  the endotherm melting enthalpy change of the microplastics ( $\text{J g}^{-1}$ ). Data is summarised in Table 5.

detailed by commercial microplastic suppliers should be verified pre-experimentation in order to have a reliable interpretation of the data. Among the analyses performed in this study to characterise the microplastics acquired commercially, Fourier Transform infrared (FT-IR) spectroscopy, particle size analysis (PSA) and differential scanning calorimetry (DSC) were shown to be crucial regarding the verification of physico-chemical properties of the commercially acquired microplastics. These three analyses provide detailed information that include polymer composition (microplastic type), polymer purity, median

particle size, particle size distribution (range of sizes), simulated surface area ( $S_{SPA}$ ), and thermal properties such as glass transition temperature ( $T_g$ ), melting temperature ( $T_m$ ) and degree of crystallinity ( $X_c$ ). SEM images of the particles has also been shown to be valuable in verifying the particle sizes and to evaluate the surface morphology of the micro-particles. Additional analysis such as zeta potential measurement can also bring insights to interpretate the factors affecting the adsorption of compounds on microplastics.

The  $\text{N}_2$ -BET adsorption-desorption analysis has limitations when

**Table 5**

Differential scanning calorimetry (DSC) of the microplastic types investigated, including the endotherm melting enthalpy change considering 100% crystallisation ( $\Delta H_{m,100\%}$ ) of plastics, glass transition temperature ( $T_g$ ), melting temperature ( $T_m$ ), and endotherm melting enthalpy change of microplastics ( $\Delta H_m$ ). The degree of crystallinity ( $X_c$ ) was calculated using equation (1). The glassiness of the microplastics is determined according to the  $T_g$  of the particle, when  $T_g < T_{amb}$  ( $T_{amb}$ ), the microplastic is considered a rubbery polymer, but when  $T_g > T_{amb}$  the material is considered a glassy polymer. The ambient temperature was assumed to be 25 °C. Polypropylene (PP), polyethylene (PE), polyethylene terephthalate (PET), polyamide (PA), polystyrene (PS), and polyvinyl chloride (PVC).

Plastics – ‘small’ particles	$\Delta H_{m,100\%}$ (J g <sup>-1</sup> )	$T_g$ (°C)	$T_m$ (°C)	$\Delta H_m$ (J g <sup>-1</sup> )	$X_c$ (%)	Crystallinity	Glassiness
PP	207.1	<0	145.37	65.486	32%	Semi-crystalline	Rubbery
PE	293.6	<0	102.95	44.169	15%	Semi-crystalline	Rubbery
PET	140.1	81.44	250.37	32.882	23%	Semi-crystalline	Glassy
PA	230.1 <sup>b</sup>	<0	221.64	51.938	23%	Semi-crystalline	Rubbery
PS	–	95.32	–	–	0	Amorphous	Glassy
PVC	–	83.72	–	–	0	Amorphous	Glassy
Plastics – ‘large’ particles	$\Delta H_{m,100\%}$ (J g <sup>-1</sup> )	$T_g$ (°C)	$T_m$ (°C)	$\Delta H_m$ (J g <sup>-1</sup> )	$X_c$ (%)	Crystallinity	Glassiness
PP	207.1	<0	160.94	96.643	47%	Semi-crystalline	Rubbery
PE	293.6	<0	104.67	49.473	17%	Semi-crystalline	Rubbery
PET	140.1	80.87	247.12	26.325	19%	Semi-crystalline	Glassy
PA	–	21.62; 93.62	–	–	0	Amorphous	Rubbery; Glassy
PS	–	96.21	–	–	0	Amorphous	Glassy
PVC	–	83.48	–	–	0	Amorphous	Glassy

- not applicable for amorphous polymers.

<sup>a</sup> Values obtained from PerkinElmer Technical Bulletin (PerkinElmer, 2000).

<sup>b</sup> Treated as nylon 6 (PA6).

applied in plastic samples. The degassing of the N<sub>2</sub>-BET adsorption-desorption analysis is normally employed at over 130 °C (Hui et al., 2021; Hussain et al., 2010). However, due to the low melting temperature of the plastics, degassing was performed at lower temperatures (30 °C; Moura et al., 2022). This adaptation of the methodology can prevent full removal of N<sub>2</sub> during the degassing step, meaning that the data might not be accurate, therefore the  $S_{BET}$  of microplastics might be often underestimated. Moreover, although the x-ray diffraction (XRD) analysis can be used to identify polymeric materials, it does not bring additional information to either the FT-IR analysis for polymer identification or to the DSC analysis regarding the degree of crystallinity of microplastics.

## 5. Limitations of the study

The current study highlights the importance of the characterisation of commercial microplastics prior to adsorption experiments. However, there were some limitations to this study. For example, the number (n = 21) of studies selected in the evaluation of the literature with respect to characterisation of microplastics does not include all microplastic adsorption studies published in recent years. The selection is a representation of what has been published in the literature. However, these studies clearly demonstrate that in the published literature there is a lack of microplastic characterisation prior to experimentation.

The current study focussed on the importance of fully understanding the properties of microplastics used in adsorption studies. However, the lack of characterisation is relevant to all microplastic-related research. Commercial microplastics have been used in various applications; from the evaluation of the impact of microplastics on wildlife (Schwarzer et al., 2022) to their use as a positive control in a study that detected microplastics in the lamprey gastrointestinal tract (Rendell-bhatti et al., 2023). Almost 400 studies relating to the adsorption of pollutants onto microplastics were published in 2022 according to the Web of Science database (2023). This illustrates the importance of the topic and the urgency to address the need for standardised microparticles and associated criteria for the characterisation of any microparticles used in a research project.

The microplastics were acquired from a single supplier. Acquiring a range of types and sizes of commercial microplastics at the required amount for an extensive characterisation analysis comes with high costs. It is important to highlight that the data from one supplier does not

necessarily represent the situation with respect to other microplastic manufactures. However, the current study highlights that any commercially acquired microplastics should be characterised prior to any experimentation to ensure reliable interpretation of data.

## 6. Conclusions

A detailed characterisation of six virgin microplastic types (PP, PE, PET, PA, PS, and PVC) acquired as two distinct sizes from a commercial source was performed. The characterisation included confirmation of the polymeric material and the determination of the crystalline structure, the degree of crystallinity, the glassiness, the particle size distribution, surface morphology, and surface area of the microplastics. Results obtained highlighted the importance of a detailed analysis of microplastics acquired commercially prior to experimentation and the need for standardised microparticles. Concerningly, it is apparent from the current work that the majority of the information provided by the supplier was inconsistent with the data obtained in the laboratory. For example, the probable presence of a grafting agent in the small particles of PP, while absent in the large particles of PP, can complicate the interpretation when assessing the impact of the particle size of PP during experiments involving microplastics. Furthermore, small and large PA showed very similar particle size distributions. In addition, one was determined to be semi-crystalline while the other was an amorphous PA. The size and the type of microplastics have been reported to be a key factor in various microplastic-related research. The current study has demonstrated that the information provided by microplastic suppliers should not be blindly trusted. While the results presented in the current study only apply to products from one supplier, this might be an indication of a more widespread issue; thus pre-characterisation of commercially acquired plastic particles is critically important when used in scientific research. Ultimately, a suite of analyses that should be undertaken on microplastics prior to their use in microplastic-related studies, including adsorption experiments, is recommended and includes Fourier transform infrared (FT-IR) spectroscopy, particle size analysis (PSA), differential scanning calorimetry (DSC), and scanning electron microscopic (SEM) imaging. Without proper characterisation of the microplastic, any data on the adsorption of chemicals by the particles must be viewed with some caution.

## Author statement

Diana S. Moura: Investigator, Writing - Original Draft, Visualization, Carlos J. Pestana: Conceptualization, Writing - Review & Editing, Supervision, Funding acquisition, Project administration, Colin F. Moffat: Resources, Writing - Review & Editing, Supervision, Jianing Hui: Methodology, John T. S. Irvine: Methodology, Linda A. Lawton: Conceptualization, Writing - Review & Editing, Supervision, Project administration.

## Declaration of competing interest

The authors declare that they have no known competing financial interests or personal relationships that could have appeared to influence the work reported in this paper.

## Data availability

Data will be made available on request.

## Acknowledgements

The authors would like to thank the Hydro Nation Scholar Programme funded by the Scottish Government through the Scottish Funding Council and managed by the Hydro Nation International Centre for funding this research. The authors would like to thank the Engineering and Physical Sciences Research Council (EPSRC) [EP/P029280/1]. In addition, the authors would like to thank Len Montgomery for proof-reading the manuscript.

## Appendix A. Supplementary data

Supplementary data to this article can be found online at <https://doi.org/10.1016/j.chemosphere.2023.138691>.

## References

- Alimi, O.S., Hernandez, L.M., Tufenkji, N., 2018. Microplastics and nanoplastics in aquatic environments: aggregation, deposition, and enhanced contaminant transport. *Environ. Sci. Technol.* 52, 1704–1724. <https://doi.org/10.1021/acs.est.7b05559>.
- An, D., Na, J., Song, J., Jung, J., 2021. Size-dependent chronic toxicity of fragmented polyethylene microplastics to *Daphnia magna*. *Chemosphere* 271, 129591. <https://doi.org/10.1016/j.chemosphere.2021.129591>.
- Atugoda, T., Vithanage, M., Wijesekara, H., Bolan, N., Sarmah, A.K., Bank, M.S., You, S., Ok, Y.S., 2021. Interactions between microplastics, pharmaceuticals and personal care products: implications for vector transport. *Environ. Int.* <https://doi.org/10.1016/j.envint.2020.106367>.
- Atugoda, T., Wijesekara, H., Werrellagama, D.R.I.B., Jinadasa, K.B.S.N., Bolan, N.S., Vithanage, M., 2020. Adsorptive interaction of antibiotic ciprofloxacin on polyethylene microplastics: implications for vector transport in water. *Environ. Technol. Innov.* 19, 100971 <https://doi.org/10.1016/j.eti.2020.100971>.
- Brown, D., 2014. Acrylic acid. *Encycl. Toxicol.* 74–75. <https://doi.org/10.1016/B978-0-12-386454-3.00220-7>.
- Cai, C., Shi, Q., Li, L., Zhu, L., Yin, J., 2008. Grafting acrylic acid onto polypropylene by reactive extrusion with pre-irradiated PP as initiator. *Radiat. Phys. Chem.* 77, 370–372. <https://doi.org/10.1016/J.RADPHYSICHEM.2007.02.081>.
- Chawla, K.K., 2012. *Composite Materials: Science and Engineering*, third ed. Springer Verlag, New York.
- Chen, X., Gu, X., Bao, L., Ma, S., Mu, Y., 2021. Comparison of adsorption and desorption of triclosan between microplastics and soil particles. *Chemosphere* 263, 127947. <https://doi.org/10.1016/j.chemosphere.2020.127947>.
- Chen, J., Sawyer, N., Regan, L., 2013. Protein–protein interactions: General trends in the relationship between binding affinity and interfacial buried surface area. *Protein Sci.* 22, 510. <https://doi.org/10.1002/PRO.2230>.
- Crawford, C.B., Quinn, B., 2017. *Microplastic Pollutants*. Elsevier Ltd, Amsterdam.
- Elizalde-velázquez, A., Subbiah, S., Anderson, T.A., Green, M.J., Zhao, X., Cañas-carrell, J.E., 2020. Sorption of three common nonsteroidal anti-inflammatory drugs (NSAIDs) to microplastics. *Sci. Total Environ.* 715, 136974 <https://doi.org/10.1016/j.scitotenv.2020.136974>.
- Fan, X., Zou, Y., Geng, N., Liu, J., Hou, J., Li, D., Yang, C., Li, Y., 2021. Investigation on the adsorption and desorption behaviors of antibiotics by degradable MPs with or without UV ageing process. *J. Hazard Mater.* 401, 123363 <https://doi.org/10.1016/j.jhazmat.2020.123363>.
- Geil, P.H., 2017. Polymer characterization. *Mod. Text. Charact. Methods*. <https://doi.org/10.1201/9780203746684>.
- Gong, X., Wang, Y., Huang, Y., Zhang, J., 2022. Effects of microplastics of different sizes on the *Chlorella vulgaris* - ganoderma lucidum co-pellets formation processes. *Sci. Total Environ.* 820, 153266 <https://doi.org/10.1016/J.SCITOTENV.2022.153266>.
- Guo, X., Chen, C., Wang, J., 2019. Sorption of sulfamethoxazole onto six types of microplastics. *Chemosphere* 228, 300–308. <https://doi.org/10.1016/j.chemosphere.2019.04.155>.
- Guo, X., Pang, J., Chen, S., Jia, H., 2018. Sorption properties of tylosin on four different microplastics. *Chemosphere* 209, 240–245. <https://doi.org/10.1016/J.CHEMOSPHERE.2018.06.100>.
- Guo, X., Wang, J., 2019. Sorption of antibiotics onto aged microplastics in freshwater and seawater. *Mar. Pollut. Bull.* 149, 110511 <https://doi.org/10.1016/J.MARPOLBUL.2019.110511>.
- Hamid, F., Akhbar, S., Halim, K.H.K., 2013. Mechanical and thermal properties of polyamide 6/HDPE-g-MAH/high density polyethylene. *Procedia Eng.* 68, 418–424. <https://doi.org/10.1016/j.proeng.2013.12.201>.
- Hüffer, T., Hofmann, T., 2016. Sorption of non-polar organic compounds by micro-sized plastic particles in aqueous solution. *Environ. Pollut.* 214, 194–201. <https://doi.org/10.1016/J.ENVPOL.2016.04.018>.
- Hüffer, T., Weniger, A.K., Hofmann, T., 2018. Sorption of organic compounds by aged polystyrene microplastic particles. *Environ. Pollut.* 236, 218–225. <https://doi.org/10.1016/J.ENVPOL.2018.01.022>.
- Hui, J., Pestana, C.J., Caux, M., Gunaratne, H.Q.N., Edwards, C., Robertson, P.K.J., Lawton, L.A., Irvine, J.T.S., 2021. Graphitic-C3N4 coated floating glass beads for photocatalytic destruction of synthetic and natural organic compounds in water under UV light. *J. Photochem. Photobiol. Chem.* 405, 112935 <https://doi.org/10.1016/J.JPHOTOCHEM.2020.112935>.
- Hussain, M., Ceccarelli, R., Marchisio, D.L., Fino, D., Russo, N., Geobaldo, F., 2010. Synthesis, characterization, and photocatalytic application of novel TiO2 nanoparticles. *Chem. Eng. J.* 157, 45–51. <https://doi.org/10.1016/J.CEJ.2009.10.043>.
- Joo, S.H., Liang, Y., Kim, M., Byun, J., Choi, H., 2021. Microplastics with adsorbed contaminants: mechanisms and treatment. *Environ. Challenges* 3, 100042. <https://doi.org/10.1016/J.ENVC.2021.100042>.
- Kausar, A., 2017. Physical properties of hybrid polymer/clay composites. *Hybrid Polym. Compos. Mater. Prop. Characterisation* 115–132. <https://doi.org/10.1016/B978-0-08-100787-7.00005-6>.
- Li, J., Zhang, K., Zhang, H., 2018. Adsorption of antibiotics on microplastics. *Environ. Pollut.* 237, 460–467. <https://doi.org/10.1016/J.ENVPOL.2018.02.050>.
- Li, Y., Li, M., Li, Z., Yang, L., Liu, X., 2019. Effects of particle size and solution chemistry on Triclosan sorption on polystyrene microplastic. *Chemosphere* 308–314. <https://doi.org/10.1016/j.chemosphere.2019.05.116>.
- Lima, M.F.S., Vasconcellos, M.A.Z., Samios, D., 2002. Crystallinity changes in plastically deformed isotactic polypropylene evaluated by x-ray diffraction and differential scanning calorimetry methods. *J. Polym. Sci., Part B: Polym. Phys.* 40, 896–903. <https://doi.org/10.1002/POLB.10159>.
- Lionetto, F., Esposito Corcione, C., 2021. An overview of the sorption studies of contaminants on poly(Ethylene terephthalate) microplastics in the marine environment. *J. Mar. Sci. Eng.* 9 <https://doi.org/10.3390/jmse9040445>.
- Liu, G., Zhu, Z., Yang, Y., Sun, Y., Yu, F., Ma, J., 2019. Sorption behavior and mechanism of hydrophilic organic chemicals to virgin and aged microplastics in freshwater and seawater. *Environ. Pollut.* 246, 26–33. <https://doi.org/10.1016/J.ENVPOL.2018.11.100>.
- Liu, P., Lu, K., Li, J., Wu, X., Qian, L., Wang, M., Gao, S., 2020. Effect of aging on adsorption behavior of polystyrene microplastics for pharmaceuticals: adsorption mechanism and role of aging intermediates. *J. Hazard Mater.* 384, 121193 <https://doi.org/10.1016/j.jhazmat.2019.121193>.
- Lu, J., Wu, Jie, Wu, Jun, Zhang, C., Luo, Y., 2020. Adsorption and desorption of steroid hormones by microplastics in seawater. *Bull. Environ. Contam. Toxicol.* 1, 3. <https://doi.org/10.1007/s00128-020-02784-2>.
- Ma, J., Zhao, J., Zhu, Z., Li, L., Yu, F., 2019. Effect of microplastic size on the adsorption behavior and mechanism of triclosan on polyvinyl chloride. *Environ. Pollut.* 254, 113104 <https://doi.org/10.1016/j.envpol.2019.113104>.
- Magadini, D.L., Goes, J.I., Ortiz, S., Lipscomb, J., Pitiranggon, M., Yan, B., 2020. Assessing the sorption of pharmaceuticals to microplastics through in-situ experiments in New York City waterways. *Sci. Total Environ.* 729, 138766 <https://doi.org/10.1016/j.scitotenv.2020.138766>.
- Mamitiana, R., Ding, J., Zhang, S., Jiang, H., Zou, H., 2018. Sorption and desorption of selected pharmaceuticals by polyethylene microplastics. *Mar. Pollut. Bull.* 136, 516–523. <https://doi.org/10.1016/j.marpolbul.2018.09.048>.
- Mandal, D.K., Bhunia, H., Bajpai, P.K., Kushwaha, J.P., Chaudhari, C.V., Dubey, K.A., Varshney, L., 2017. Optimization of acrylic acid grafting onto polypropylene using response surface methodology and its biodegradability. *Radiat. Phys. Chem.* 132, 71–81. <https://doi.org/10.1016/J.RADPHYSICHEM.2016.12.003>.
- Moura, D.S., Pestana, C.J., Moffat, C.F., Hui, J., Irvine, J.T.S., Edwards, C., Lawton, L.A., 2022. Adsorption of cyanotoxins on polypropylene and polyethylene terephthalate: microplastics as vector of eight microcystin analogues. *Environ. Pollut.* 303, 119135 <https://doi.org/10.1016/j.envpol.2022.119135>.
- Müller, C.M., Pejčić, B., Esteban, L., Piane, C.D., Raven, M., Mizaikoff, B., 2014. Infrared attenuated total reflectance spectroscopy: an innovative strategy for analyzing mineral components in energy relevant systems. *Sci. Rep.* 4, 1–11. <https://doi.org/10.1038/srep06764>, 2014.
- PerkinElmer application note, 2000. DSC as Problem Solving Tool: Measurement of Percent Crystallinity of Thermoplastics [WWW Document]. URL. <https://resources>.



- [perkinelmer.com/corporate/content/applicationnotes/app\\_thermalcrystallinitythermoplastics.pdf](http://perkinelmer.com/corporate/content/applicationnotes/app_thermalcrystallinitythermoplastics.pdf).
- Pestana, C., Moura, D.S., Capelo-Neto, J., Edwards, C., Dreisbach, D., Spengler, B., Lawton, L., 2021. Potentially poisonous plastic particles: microplastics as a vector for cyanobacterial toxins microcystin-LR and microcystin-LF. *Environ. Sci. Technol.* 55, 15940–15949. <https://doi.org/10.1021/acs.est.1c05796>.
- Puckowski, A., Cwięk, W., Mioduszevska, K., Stepnowski, P., Białk-Bielińska, A., 2021. Sorption of pharmaceuticals on the surface of microplastics. *Chemosphere* 263, 127976. <https://doi.org/10.1016/j.chemosphere.2020.127976>.
- Razanajatovo, R.M., Ding, J., Zhang, S., Jiang, H., Zou, H., 2018. Sorption and desorption of selected pharmaceuticals by polyethylene microplastics. *Mar. Pollut. Bull.* 136, 516–523. <https://doi.org/10.1016/j.marpolbul.2018.09.048>.
- Rendell-bhatti, F., Bull, C., Cross, R., Cox, R., Adediran, G.A., 2023. From the environment into the biomass : microplastic uptake in a protected lamprey species. *Environ. Pollut.* 323, 121267 <https://doi.org/10.1016/j.envpol.2023.121267>.
- Schwarzer, M., Brehm, J., Vollmer, M., Jasinski, J., Xu, C., Zainuddin, S., Fröhlich, T., Schott, M., Greiner, A., Scheibel, T., Laforsch, C., 2022. Shape, size, and polymer dependent effects of microplastics on *Daphnia magna*. *J. Hazard Mater.* 426, 128136 <https://doi.org/10.1016/J.JHAZMAT.2021.128136>.
- Seki, A., Koike, Y., Yamamoto, M., Tohyama, K., Sample, A., 2014. High field dielectric properties of polyethylene terephthalate. In: *Conference on Electrical Insulation and Dielectric Phenomena High*, pp. 546–549.
- Seo, C., Lee, J.W., Jung, W.-K., Lee, Y.-M., Lee, S., Lee, S.G., 2022. Examination of Microcystin Adsorption by the Type of Plastic Materials Used during the Procedure of Microcystin Analysis. <https://doi.org/10.3390/toxins14090625>.
- Singh, M.K., Singh, A., 2022. Thermal characterization of materials using differential scanning calorimeter. *Charact. Polym. Fibres* 201. <https://doi.org/10.1016/B978-0-12-823986-5.00006-3>. –222.
- Speakman, S.A., 2021. Introduction to X-Ray Powder Diffraction Data Analysis [WWW Document]. *Cent. Mater. Sci. Eng. MIT.* URL. <http://prism.mit.edu/xray/>
- Thompson, R.C., Swan, S.H., Moore, C.J., Vom Saal, F.S., 2009. Our plastic age. *Philos. Trans. R. Soc. B Biol. Sci.* 364, 1973–1976. <https://doi.org/10.1098/rstb.2009.0054>.
- Turner, A., Holmes, L.A., 2015. Adsorption of trace metals by microplastic pellets in fresh water. *Environ. Chem.* 12, 600–610. <https://doi.org/10.1071/EN14143>.
- Vaughan, R., Turner, S.D., Rose, N.L., 2017. Microplastics in the sediments of a UK urban lake. *Environ. Pollut.* 229, 10–18. <https://doi.org/10.1016/j.envpol.2017.05.057>.
- Wagner, M., Scheger, C., Alvarez-Munoz, D., Brehnholt, N., Bourrain, X., Buchinger, S., Fries, E., Grosbois, C., Klasmeier, J., Marti, T., Rodriguez-Mozaz, S., Urbatzka, R., Vethaak, A.D., Winther-Nielsen, M., Reifferscheid, G., 2014. Microplastics in freshwater ecosystems: what we know and what we need to know. *Environ. Sci. Eur.* 26, 1–9.
- Wagstaff, A., Lawton, L.A., Petrie, B., 2022. Polyamide microplastics in wastewater as vectors of cationic pharmaceutical drugs. *Chemosphere* 288, 132578. <https://doi.org/10.1016/J.CHEMOSPHERE.2021.132578>.
- Wagstaff, A., Petrie, B., 2022. Enhanced desorption of fluoxetine from polyethylene terephthalate microplastics in gastric fluid and sea water. *Environ. Chem. Lett.* 1, 1–8. <https://doi.org/10.1007/S10311-022-01405-0>, 2022.
- Wang, F., Wong, C.S., Chen, D., Lu, X., Wang, Fei, Zeng, E.Y., 2018a. Interaction of toxic chemicals with microplastics : a critical review. *Water Res.* 139, 208–219. <https://doi.org/10.1016/j.watres.2018.04.003>.
- Wang, W., Yuan, W., Chen, Y., Wang, J., 2018b. Microplastics in surface waters of dongting lake and hong lake, China. *Sci. Total Environ.* 633, 539–545. <https://doi.org/10.1016/j.scitotenv.2018.03.211>.
- Wu, C., Zhang, K., Huang, X., Liu, J., 2016. Sorption of pharmaceuticals and personal care products to polyethylene debris. *Environ. Sci. Pollut. Res.* 23, 8819–8826. <https://doi.org/10.1007/s11356-016-6121-7>.
- Wu, D., Wang, T., Wang, J., Jiang, L., Yin, Y., Guo, H., 2021. Size-dependent toxic effects of polystyrene microplastic exposure on *Microcystis aeruginosa* growth and microcystin production. *Sci. Total Environ.* 761, 143265 <https://doi.org/10.1016/j.scitotenv.2020.143265>.
- Wu, J., Xu, P., Chen, Q., Ma, D., Ge, W., Jiang, T., 2020. Effects of polymer aging on sorption of 2,20,4,40-tetrabromodiphenyl ether by polystyrene microplastics. *Chemosphere* 253, 126706. <https://doi.org/10.1016/j.chemosphere.2020.126706>.
- Wu, X., Liu, P., Huang, H., Gao, S., 2020. Adsorption of triclosan onto different aged polypropylene microplastics: critical effect of cations. *Sci. Total Environ.* 717, 137033 <https://doi.org/10.1016/J.SCIOTOTENV.2020.137033>.
- Xiong, X., Zhang, K., Chen, X., Shi, H., Luo, Z., Wu, C., 2018. Sources and distribution of microplastics in China's largest inland lake – qinghai Lake. *Environ. Pollut.* 235, 899–906. <https://doi.org/10.1016/j.envpol.2017.12.081>.
- Xu, B., Liu, F., Brookes, P.C., Xu, J., 2018a. Microplastics play a minor role in tetracycline sorption in the presence of dissolved organic matter. *Environ. Pollut.* 240, 87–94. <https://doi.org/10.1016/J.ENVPOL.2018.04.113>.
- Xu, B., Liu, F., Brookes, P.C., Xu, J., 2018b. The sorption kinetics and isotherms of sulfamethoxazole with polyethylene microplastics. *Mar. Pollut. Bull.* 131, 191–196. <https://doi.org/10.1016/j.marpolbul.2018.04.027>.
- Xu, X., Chen, S., Zhuang, L., Zheng, C., Wu, Y., 2014. Establishment of a novel surface-imprinting system for melamine recognition and mechanism of template-matrix interactions. *J. Mater. Sci.* 49, 2853–2863. <https://doi.org/10.1007/S10853-013-7991-4/FIGURES/14>.
- Yang, G.L., Zhang, C.Y., Tan, L.C., Zhang, X.H., 2013. The effect of specific surface area on the solid grafting reaction of maleic anhydride-grafted polypropylene. *Adv. Mater. Res.* 781–784, 385–389. <https://doi.org/10.4028/www.scientific.net/AMR.781-784.385>.
- Yu, F., Li, Y., Huang, G., Yang, C., Chen, C., Zhou, T., Zhao, Y., Ma, J., 2020. Adsorption behavior of the antibiotic levofloxacin on microplastics in the presence of different heavy metals in an aqueous solution. *Chemosphere* 260, 127650. <https://doi.org/10.1016/J.CHEMOSPHERE.2020.127650>.
- Zhang, H., Wang, J., Zhou, B., Zhou, Y., Dai, Z., Zhou, Q., Christie, P., Luo, Y., 2018. Enhanced adsorption of oxytetracycline to weathered microplastic polystyrene: kinetics, isotherms and influencing factors. *Environ. Pollut.* 243, 1550–1557. <https://doi.org/10.1016/j.envpol.2018.09.122>.